Synthesis and Crystallization of Syndiotactic Random Copolymers of Styrene and *p*-*n*-Butylstyrene and of Syndiotactic Poly(*p*-*n*-butylstyrene)

Ralf Thomann, Friedrich G. Sernetz, Johannes Heinemann, Sandra Steinmann, and Rolf Mülhaupt

Freiburger Materialforschungszentrum und Institut für Makromolekulare Chemie der Albert-Ludwigs-Universität Freiburg, Stefan-Meier-Strasse 21, D-79104 Freiburg, Germany

Jörg Kressler*

Martin-Luther-Universität Halle-Wittenberg, Fachbereich Werkstoffwissenschaften, 06099 Halle (Saale), Germany

Received August 5, 1997; Revised Manuscript Received October 21, 1997[⊗]

ABSTRACT: The metallocene-catalyzed syndiospecific synthesis of the new homopolymer of *p*-*n*-butylstyrene and its random copolymers with styrene is reported. The crystalline morphology of the resulting polymers is studied by means of atomic force microscopy (AFM), wide-angle X-ray scattering (WAXS), differential scanning calorimetry (DSC), and light microscopy. Copolymers with relatively small *p*-*n*-butylstyrene content are crystallizable from the melt. It is shown that under these crystallization conditions the α-modification is favored relative to the *β*-modification (both modifications known from syndiotactic polystyrene) with increasing *p*-*n*-butylstyrene content. The crystalline morphology is built up by crystalline slices formed by broad lamellae. The equilibrium melting temperature of the copolymers decreases with increasing *p*-*n*-butylstyrene content. Furthermore, the crystallization of quenched, amorphous samples during thermal annealing below the melting temperatures (cold crystallization) or induced by solvents is studied. The syndiotactic *p*-*n*-butylstyrene homopolymer has two modifications characterized by WAXS which are different from all modifications of syndiotactic polystyrene or syndiotactic *p*-methylstyrene homopolymer.

Introduction

Since the first synthesis of syndiotactic polystyrene (s-PS) by Ishihara et al. in 1986,[1] a large variety of early transition metal complexes promoting syndiospecific styrene polymerization have been developed.[2−9] In contrast to metallocene-catalyzed aliphatic α-olefin polymerization, the insertion step for styrene[10] is known to proceed via secondary insertion.[2b] Syndiospecific homo- and copolymerization has been carried out so far using methyl-substituted or halogenated styrenes, resulting in significant differences in the copolymerization parameters of activated or deactivated styrenes with respect to styrene.[11,12]

Syndiotactic polystyrene (s-PS) has a complex polymorphism. Three different crystal structures (α, *β*, *γ*) and one clathrate structure (*δ*) have been described.[13−15] Furthermore, the two crystalline modifications α and *β* are divided in different submodifications having different degrees of structural order (α′, α″, *β*′, *β*″).[13,14] The α′- and α″-forms contain planar zigzag chains with an identity period $c = 0.51$ nm (conformation $(tt)_n$). The packing of the phenyl rings is similar to that of isotactic polystyrene.[16] The phenyl groups in the two α-forms are arranged in a rhombohedral manner. The polymer backbones satisfy a rhombohedral symmetry only in the α″-modification. The polymer backbones in the α′-form are statistically disordered.[14] The *β*′- and *β*″-forms contain also planar zigzag chains. In both forms the chains are packed in a orthorhombic lattice. Again the *β*′-form shows a limited statistical disorder.[13] The third crystalline form (*γ*) and the clathrate modification (*δ*) contain (2/1)2 helices with an identity period of $c = 0.78$ nm.[15] In syndiotactic copolymers of styrene and *p*-methylstyrene, the α-modification is favored relative to the *β*-modification.[18,19]

This contribution deals with the metallocene-catalyzed syndiospecific copolymerization of styrene and *p*-*n*-butylstyrene (BuS). This is a model system in order to study the influence of longer aliphatic substitution on the phenyl ring on both copolymerization behavior and crystal structure of the resulting copolymers. Therefore, the crystallization behavior of the copolymers (s-P(S-*co*-BuS)-X, X ≡ mol % BuS) and the poly(*p*-*n*-butylstyrene) homopolymer (s-P(BuS)) is studied by means of atomic force microscopy (AFM), wide-angle X-ray scattering (WAXS), differential scanning calorimetry (DSC), and light microscopy.

Experimental Section

Materials. $CpTiCl_3$ (Cp = cyclopentadienyl) was purchased from Aldrich and purified by sublimation. All manipulations involving air and moisture sensitive compounds were carried out under dry argon atmosphere, using Schlenk tube and glovebox techniques. Methylalumoxane (MAO) was provided by Witco GmbH as a 10 wt % solution in toluene. Toluene (Roth, p.a., >99,7%) was purified by passing it through a column with acidic Al_2O_3, distilled over $LiAlH_4$/BuLi and refluxed over Na/K alloy, from which it was freshly distilled prior to use. Styrene (Fluka, > 99%) was purified by distillation over $LiAlH_4$ and stored under argon at 0 °C.

Monomer Synthesis. The monomer BuS was synthesized from butylbenzene according to literature, with the intermediate products 4-butyl-1-acetylbenzene and 1-(4−butylphenyl)-ethan-1-ol.[24] Table 1 summarizes the ^{1}H-NMR data of BuS and of the intermediate products.

Polymerizations. Polymerizations were carried out in a 100 mL Schlenk flask. The flask was filled with toluene, styrene, BuS and a part of the methylalumoxane (MAO) needed. The metallocene solution (in 10 wt % MAO solution) was then injected into the flask, so that an in situ start of the

* To whom correspondence should be addressed.

[⊗] Abstract published in *Advance ACS Abstracts,* December 1, 1997.

S0024-9297(97)01185-6 CCC: $14.00

Table 1. ^{1}H-NMR Data of BuS and Intermediate Products

Material	^{1}H-NMR (δ (ppm))
4-butyl-1-acetyl-benzene	7.80 (d, 2H), 7.20 (d, 2H), 2.60 (t, 2H), 2.50 (s, 3H), 1.55 (quintet, 2H), 1.30 (sextet, 2H), 0.85 (t, 3H)
1-(4-butylphenyl)-ethan-1-ol	7.3 (d, 2H), 7.2 (d, 2H), 4.9 (q, 1H), 2.6 (t, 2H), 1.6 (s, 1H), 1.6 (quintet, 2H), 1.5 (d, 3H), 1.4 (sextet, 2H), 0.95 (t, 3H)
n-butylstyrene	7.15 (d, 2H), 6.95 (d, 2H), 6.50 (q, 1H), 5.50 (d, 1H, cis), 5.00 (d, 1H, trans), 2.40 (t, 2H), 1.40 (quintet, 2H), 1.15 (sextet, 2H), 0.75 (t, 3H)

polymerization was achieved. Further polymerization conditions are given in Table 2. Polymerizations were stopped by injecting C_3H_7OH. The polymers were precipitated by pouring into 500 mL of acidic (10 mL of half-concentrated HCl) CH_3-OH, filtered and dried under vacuum to constant weight.

Polymer Characterization. NMR spectra were recorded on a Bruker ARX 300 spectrometer operating at 300 MHz for ^{1}H and at 75.4 MHz for ^{13}C. Spectra were taken at 100 °C using $C_2D_2Cl_4$ as solvent. The chemical shifts are reported in ppm vs tetramethylsilane (TMS). Signals were assigned according to literature data.[23] Molecular weights and molecular weight distributions reported were determined by high temperature gel permeation chromatography (GPC) calibrated with polystyrene standards. Differential scanning calorimetry (DSC) was performed on a Perkin-Elmer DSC-7 thermal analyzer using a heating rate of 20 °C/min.

Light Microscopy. The light microscopic investigations are carried out with an Olympus-Vanox AH2 microscope and a Linkam TMS 90 hot stage that allows observation during isothermal crystallization. The samples used to study the crystalline morphology were prepared by melting the powder of the as-prepared and dried polymer between two cover glasses. The layer thickness between the glasses was about 30−50 μm. The samples were held for 10 min at 280 °C and then quenched to crystallization temperature with a rate of 99 °C/min.

Atomic Force Microscopy. The prepared films were etched to remove amorphous material from the surface. The etching reagent was prepared by stirring 0.02 g of potassium permanganate in a mixture of 4 mL of sulfuric acid (95−97%) and 10 g of orthophosphoric acid. The 30−50 μm thick films were immersed into the fresh etching reagent at room temperature and held there for 1 h. At the beginning, the samples were held in an ultrasonic bath for 15 min. For subsequent washings, a mixture of two parts by volume of concentrated sulfuric acid and seven parts of water was prepared and cooled to near the freezing point with dry ice in 2-propanol. The samples were washed successively with 30% aqueous hydrogen peroxide (to remove any manganese dioxide present). Then the samples were washed with distilled water. Each washing was supported with an ultrasonic bath. The AFM experiments were carried out with a 'Nanoscope III' scanning probe microscope (Digital Instruments) under ambient conditions in the tapping-mode/height-mode (TMHM) and in the tapping-mode/amplitude-mode (TMAM).

WAXS Measurements. The measurements were carried out with a Siemens D500 apparatus. For WAXS measurements the Cu Kα radiation of a wavelength of $\lambda = 0.154$ nm was used.

Results and Discussion

Synthesis and Characterization. Employing the syndiospecific catalyst system $CpTiCl_3$/MAO, BuS was homopolymerized and copolymerized with styrene. Using a catalyst concentration of 100 μmol/L, an Al/Ti molar ratio of 2000, and a polymerization temperature of 25 °C, the styrene concentration was varied between 2.2 and 1.1 mol/L and the BuS concentration was varied between 0.03 and 0.68 mol/L. All polymer data and polymerization conditions are summarized in Table 2.

Copolymer molecular weights between $M_n = 17\,000$ and 124 000 are achieved. A trend is evident for molecular weights as a function of BuS content, as higher BuS contents in the monomer feed lower the molecular weights of the resulting copolymers. This can be explained by taking the increased electron density of BuS with respect to styrene into account. Higher electron density can result in formation of a more stable π-complex during the insertion process, resulting in a slower insertion rate for BuS. With respect to β-hydrid elimination as chain termination mechanism, this leads to lower molecular weights with increasing BuS content. Neat s-PS was kindly provided by Dr. J. Wünsch (BASF AG). The content of racemic pentads was 96% determined by ^{13}C-NMR. The M_n value was 67 000 ($M_w/M_n = 2.1$) determined by high temperature SEC using atactic polystyrene standards.

Comonomer contents were calculated using ^{1}H-NMR spectra as aromatic signals for styrene and BuS are well separated (Figure 1). The BuS content of copolymers increases rapidly with BuS concentration in the monomer feed. BuS is incorporated in amounts higher than the BuS content of the monomer feed resulting in copolymerization parameters $r_S = 0.52$ and $r_{BuS} = 1.2$ ($r_S r_{BuS} = 0.6$) obtained from Fineman-Ross plots. This is in agreement with results for styrene/*p*-methylstyrene copolymerization where a copolymerization parameter (r_{MS}) larger than 1 was also found for *p*-methylstyrene.[11]

It is known that some substituted styrenes do not give syndiotactic microstructures though using a catalyst known for syndiospecific polymerization of styrene.[11,12] Therefore, analysis of copolymer tacticity was performed from ^{1}H- and ^{13}C-NMR spectra, respectively. Figure 1 depicts ^{1}H-NMR spectra of the homopolymer s-P(BuS) as well as of copolymers with 20 and 47 mol % BuS, respectively. Separation of aromatic proton resonances with $\delta = 6.7$ and 7.2 ppm for styrene and $\delta = 6.5$ and 6.9 ppm for BuS allows for integration of the signals in

Table 2. Copolymerization of Styrene with *p-n*-Butylstyrene Using $CpTiCl_3$/MAO[a]

sample	S/BuS molar ratio (mol/mol)	[S] (mol/L)	[BuS] (mol/L)[f]	BuS content in monomer feed (mol %)	activity (kg of polymer/mol Ti·h·mol/L)	BuS content in copolymer[b] (mol %)	T_g[c] (°C)	M_n[d] × 10^3	M_w/M_n
s-P(S-*co*-BuS)-4	72	2.16	0.03	1.3	59	4	95	81	2.2
s-P(S-*co*-BuS)-7	30	2.09	0.07	3.2	87	7	93	85	2.2
s-P(S-*co*-BuS)-11	14	1.98	0.14	6.6	80	11	90	124	1.6
s-P(S-*co*-BuS)-20	7	1.75	0.27	13.8	89	20	83	33	5.6
s-P(S-*co*-BuS)-27	3.6	1.55	0.42	21.7	108	27	82	51	4.1
s-P(S-*co*-BuS)-40	2.5	1.33	0.53	29.3	94	40	66	18	6.3[e]
s-P(S-*co*-BuS)-47	1.6	1.10	0.68	38.9	90	47	61	21	7.7[e]
s-P(BuS)	0		0.68	100	183	100	33	17	5.7[e]

[a] Polymerization conditions: [cat] = 100 μmol/L, Al/Ti = 2000, T = 25 °C, t = 3 h, solvent = toluene, volume = 40 mL, and S = styrene. [b] Calculated from ^{1}H- and ^{13}C-NMR spectra. [c] By differential scanning calorimetry (DSC). [d] By gel permeation chromatography (GPC) vs polystyrene standards. [e] Broad polydispersities due to small amounts of low molecular weight polymer. [f] Density of butylstyrene = 0.88 g/cm^3.

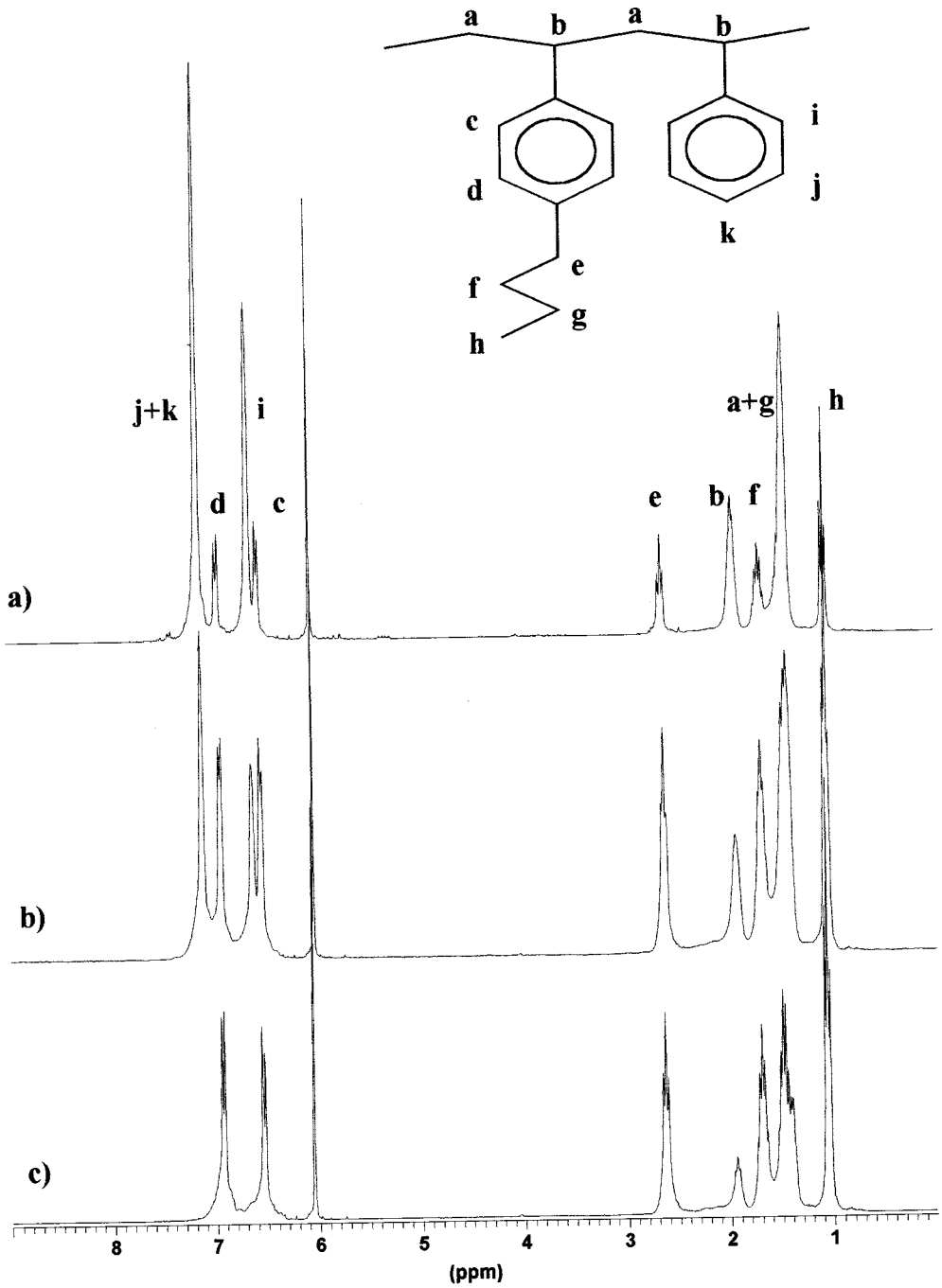

Figure 1. ^{1}H-NMR spectra ($C_2D_2Cl_4$, 300 MHz, 100 °C): (a) s-P(S-*co*-BuS)-20; (b) s-P(S-*co*-BuS)-47; (c) s-P(BuS).

order to determine copolymer composition. Assignments of all other signals are indicated. The signal for the main chain methin groups shows a shift of $\delta = 1.95$ ppm and a triplet, typical for syndiotacticity.

Figure 2 shows the aromatic region of the ^{13}C-NMR spectra of the homopolymer s-P(BuS) (top) and of the copolymer sample with 47 mol % BuS (bottom). The copolymer shows additional resonances at $\delta = 145.6$ and 125.5 ppm, assigned to the aromatic C1′ and C4′ carbon atoms of unsubstituted styrene units. It can be seen that C1 and C1′ carbon atoms of substituted and unsubstituted styrenes at $\delta = 142.7$ and 145.7 ppm, respectively, give very sharp resonances. This sharpness together with the characteristic shift indicates syndiotactic microstructures for both BuS homo- and copolymers.

Figure 3 shows the melting points and T_g values of as-prepared samples that are dried under vacuum above T_g to remove any solvent present. The melting points of the copolymers decrease rapidly with increasing BuS content. Melting points range from 270 °C for neat s-PS down to 70 °C for s-P(S-*co*-BuS)-40. The neat s-P(BuS) shows a melting point of 133 °C. This indicates the existence of an eutecticum for the melting points as a function of the copolymer composition.[25] Glass transition temperatures of copolymers were found to depend quite linearly on BuS contents. The glass transition temperature for the homopolymer s-P(BuS) is 33 °C.

Crystallization from the Melt. The melting points of the copolymers shown in Figure 3 are obtained under nonequilibrium conditions. Equilibrium melting points, $T_m°$, are determined for s-P(S-*co*-BuS)-4 and s-P(S-*co*-BuS)-7 using Hoffman−Weeks plots.[26] Copolymers with a higher content of BuS are not crystallizable from the melt. Figure 4 shows the Hoffman−Weeks plots of s-PS, s-P(S-*co*-BuS)-4, and s-P(S-*co*-BuS)-7. The nonequilibrium melting points, T_m, were determined by DSC. The point of the return of the melting endotherm to the

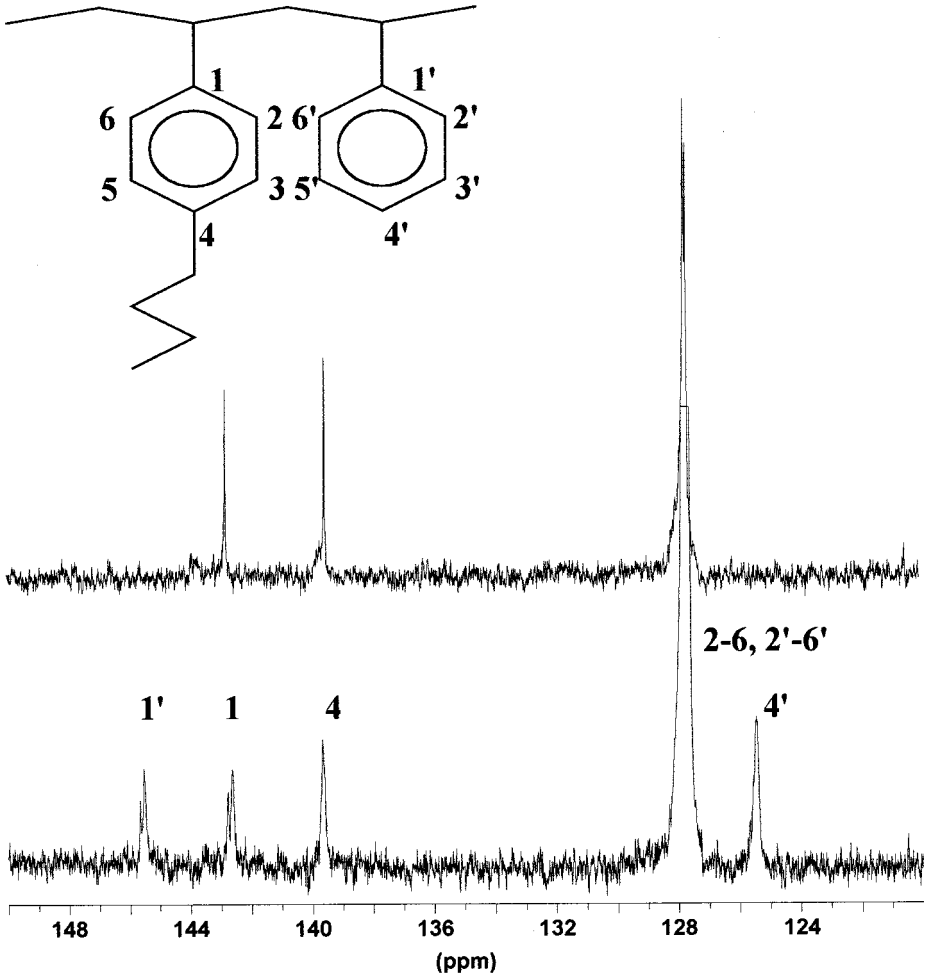

Figure 2. Aromatic region of the ^{13}C-NMR spectra ($C_2D_2Cl_4$, 75,4 MHz, 100 °C): s-P(BuS) (top); s-P(S-*co*-BuS)-47 (bottom).

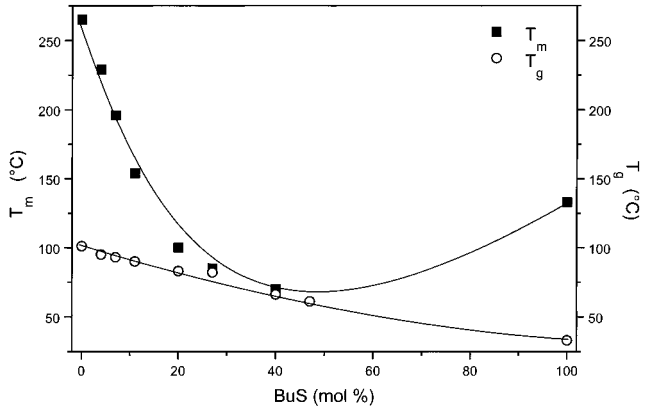

Figure 3. Melting points and glass transition temperatures of the precipitated and dried polymers obtained by DSC as a function of copolymer composition. The lines are drawn to guide the eye.

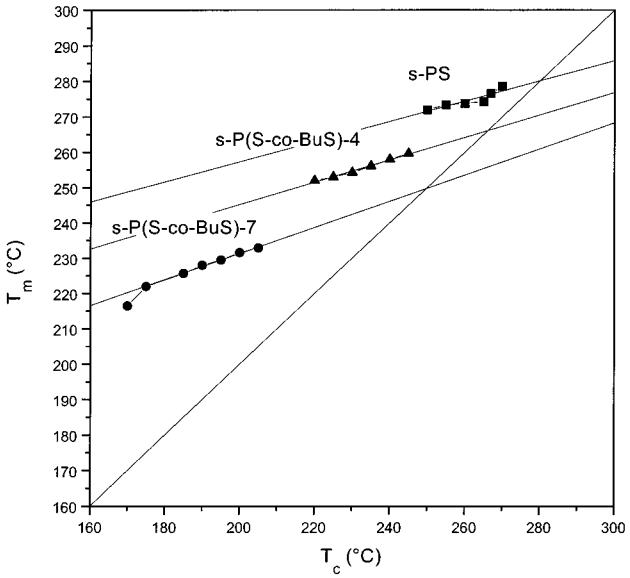

Figure 4. Hoffman−Weeks plots of s-PS, s-P(S-*co*-BuS)-4, and s-P(S-*co*-BuS)-7.

baseline is defined as the nonequilibrium melting point. This point is taken at three different heating rates for every polymer and extrapolated to a heating rate of 0 °C/min. The equilibrium melting temperatures are obtained from the intersection of the linear extrapolation with the straight line given by $T_m = T_c$. The resulting equilibrium melting points are 279 °C for s-PS homopolymer, 265 °C for s-P(S-*co*-BuS)-4 and 249 °C for s-P(S-*co*-BuS)-7. As discussed below, the equilibrium melting point of neat s-P(BuS) is 162 °C. Thus the $T_m°$ values of s-P(S-*co*-BuS)-4 and s-P(S-*co*-BuS)-7 show significant negative deviations from additivity with respect to the neat homopolymers. This again supports the possible occurrence of an eutectic behavior of the copolymer melting points.

Figure 5 shows the WAXS traces of s-P(S-*co*-BuS)-4 (a) and of s-P(S-*co*-BuS)-7 (b) isothermally crystallized from the melt at 205 °C. Furthermore, an s-P(S-*co*-BuS)-7 trace (c) obtained after crystallization at 180 °C is shown. Thus traces a and c were obtained from samples crystallized at identical supercoolings ($T_m°-T_c$). s-P(S-*co*-BuS)-4 isothermally crystallized at 205 °C

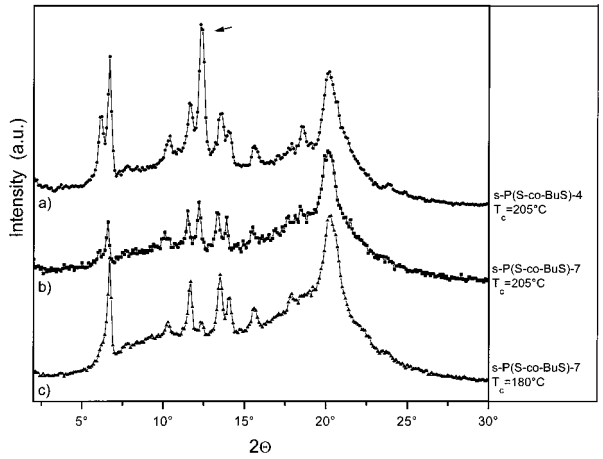

Figure 5. WAXS traces of s-P(S-*co*-BuS)-4 isothermally crystallized at 205 °C (a) and of s-P(S-*co*-BuS)-7 isothermally crystallized at 205 °C (b) and at 180 °C (c). The arrow in trace a indicates the 040 reflection of the β'-modification.

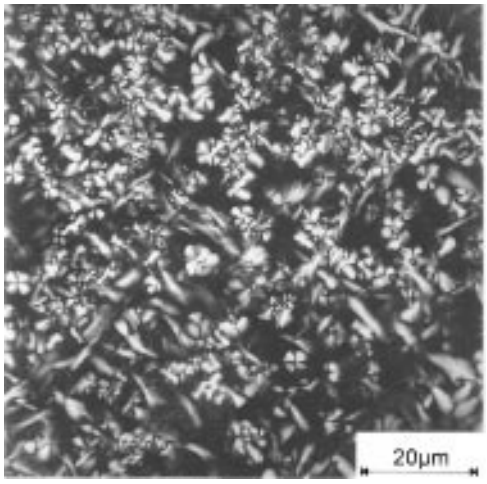

Figure 6. Light micrograph of s-P(S-*co*-BuS)-7 isothermally crystallized at 205 °C.

shows mainly the β'-modification. One intense peak of the β'-modification at $2\theta = 12.3°$ is marked with an arrow. s-P(S-*co*-BuS)-7 isothermally crystallized at the same temperature shows the α- and the β-modification. The increasing amount of the α-modification with increasing comonomer content is also observed for syndiotactic copolymers of styrene and *p*-methylstyrene.[18,19] Crystallized at 180 °C, s-P(S-*co*-BuS)-7 shows mainly the α-modification. This supports again the statement that with increasing content of BuS the α-modification is promoted. Because our WAXS measurements indicate that BuS units are not included in the crystal lattice of copolymers with high s-PS content, it can be excluded that the steric incorporation of the *n*-butyl group into the crystal lattice influences the crystal modification. Possible reasons for the increase of the α-modification can be as follows: In the case that the crystal modifications have different values of the lamella thickness (as e.g. known for isotactic polypropylene[20]), it is possible that the copolymer units influence the crystallization kinetics of the modifications to a different degree. This is related to the selection of crystallizable sequences of fitting length.[21] Further investigations on this problem have to be done especially employing small angle X-ray measurements where first results are obtained on s-PS homopolymer.[22]

Figure 6 depicts a polarized light micrograph of s-P(S-*co*-BuS)-7 isothermally crystallized at 205 °C. The appearance of elongated crystalline entities and apparently spherolitic structures is similar to s-PS homopolymer crystallized at temperatures above 245 °C. In this temperature range the crystal growth rate of s-PS homopolymer is similar to that of s-P(S-*co*-BuS)-7 at 205 °C.

Figure 7a shows an AFM micrograph of an etched sample of s-P(S-*co*-BuS)-7 isothermally crystallized at 205 °C. Crystalline entities formed by lamellae radiating from a central nucleus can be observed. These lamellae have a preferred orientation within the whole supermolecular structure. Therefore, it can be assumed that the supermolecular structure is not formed by three dimensional spherolites but from crystalline slices. Different orientations of these slices in the bulk yield the two typical appearances in the light micrograph; similar to spherolites for flat-on slices and elongated entities for edge-on slices seen in the photograph of Figure 6. Figure 7b shows an enlarged AFM micrograph of a flat-on slice. The mainly flat-on arrangement of the lamellae starts from the central nucleus. Figure 7c depicts an enlarged micrograph of an edge-on arranged slice. The lamellar structure is visible. The average lamella to lamella distance is measured to be 24 nm. The crystalline morphologies discussed above and observed by light microscopy and AFM are schematically drawn in Figure 7d. The left scheme shows a crystalline aggregate formed by flat-on lamellae as observed in the AFM micrograph in Figure 7b. This appears in polarized light micrographs similar to spherolitic structures (cf. Figure 6). The schematic drawing on the right hand side of Figure 7d symbolizes the same crystalline aggregates in the case that the lamellae can be observed edge-on. This leads to the appearance of elongated morphologies in polarized light micrographs (cf. Figure 6) and can be visualized directly by AFM as shown in Figure 7c.

Figure 8a shows an AFM micrograph of a different superstructure of s-P(S-*co*-BuS)-7 obtained after isothermal crystallization at 205 °C. Circular entities appear which can be considered as single crystals. They are built up by a single broad lamella. Figure 8b shows one of these circular entities in more detail. Again the structure is formed by a broad lamella. In the center of the structure a hole is visible. An AFM micrograph where the hole area is zoomed can be seen in Figure 8c. The lamella forms a helical structure indicating that these entities result from screw dislocations. Similar circular structures were reported for polyethylene.[27]

Quenched Amorphous Samples and Their Crystallization. Quenching of s-PS, s-P(BuS), and of the copolymers from a melt in acetone at its melting point leads to totally amorphous samples. The structure of these samples and their behavior upon thermal treatment or upon exposure to $CHCl_3$ vapor is reported in the following. For the quenched amorphous phase of neat s-PS, neat s-P(BuS), and of the copolymers the WAXS pattern shows two characteristic peaks (similar to that of the bottom trace of Figure 10). This behavior is similar to that of atactic polystyrene. For this polymer two amorphous halos in WAXS traces at $2\theta = 9.5°$ and $2\theta = 19.5°$ are generally observed.[28−32] The first explanation of these peaks was given by Katz.[32] A more detailed discussion was done by Krimm and Tobolsky.[31] They assigned the maximum of the first peak at $2\theta = 9.5°$ to the average intermolecular chain to chain distance. The maximum at $2\theta = 19.5°$ was related to intramolecular distances between the phenyl rings. Figure 9 shows the intermolecular chain to chain distance and the intramolecular distances between the phenyl rings calculated from the position of the two

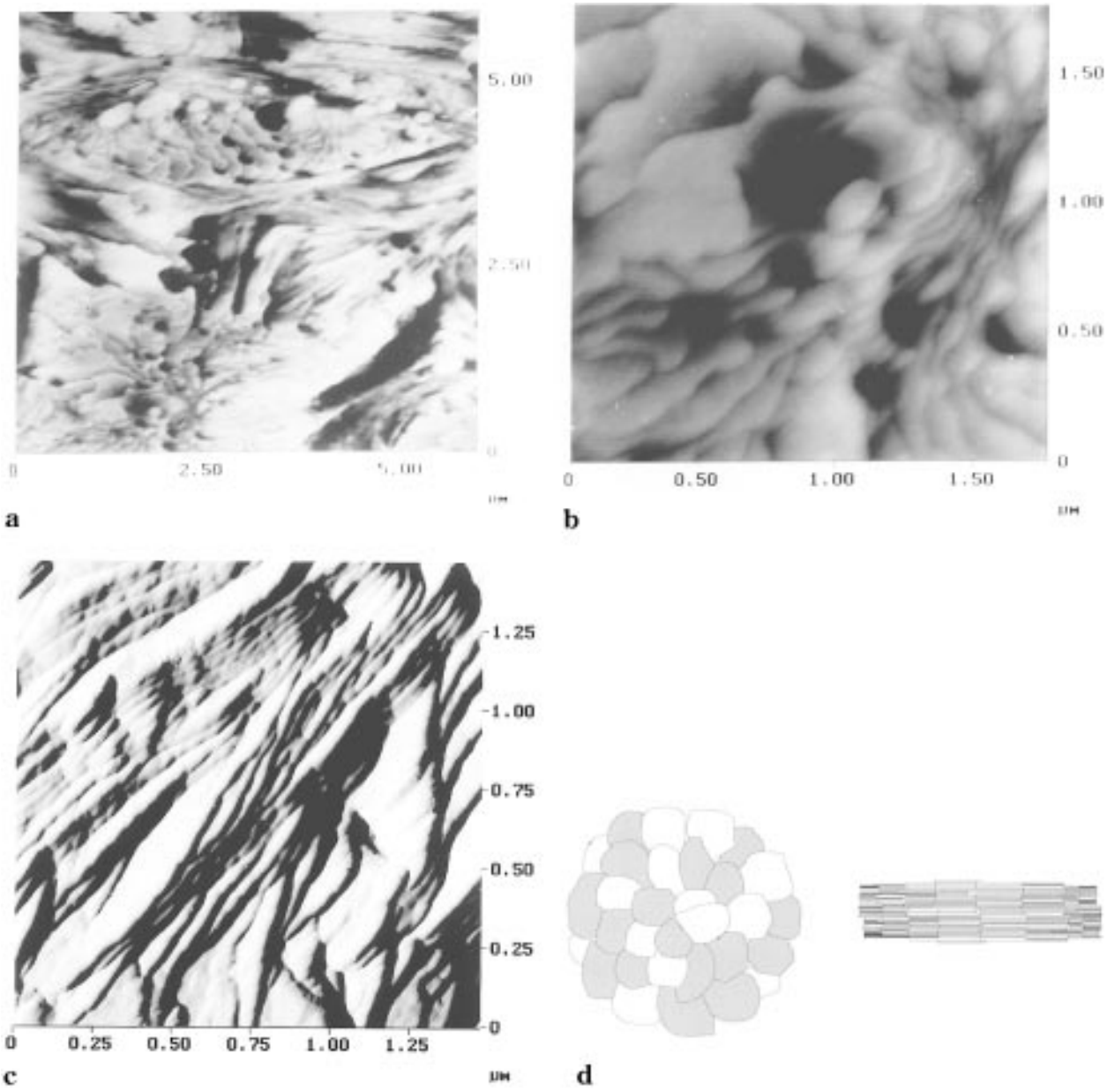

Figure 7. AFM micrographs of s-P(S-*co*-BuS)-7 isothermally crystallized at 205°: (a) crystalline entity formed by broad lamellae (TMHM); (b) from part a, center of a crystalline entity; (c) edge-on lamellae (TMAM); (d) schematic drawing of crystalline entities formed by flat-on lamellae (left) and edge-on lamellae (right).

maxima vs the BuS content. The average chain to chain distance shifts from 0.97 nm ($2\theta = 9.1°$) for neat s-PS to 1.5 nm ($2\theta = 5.3°$) for neat s-P(BuS). Hence, the chain to chain distance increases with increasing copolymer content caused by the space requirement of the long aliphatic *n*-butyl side groups. The second maximum at about $2\theta = 19°$ is nearly independent of the copolymer content. Thus the intramolecular ring to ring distance is constant indicating that there does not exist any significant change in the chain conformation.

The next part deals with the vapor-induced crystallization of quenched amorphous samples. Figure 10 shows the WAXS traces of originally amorphous copolymers after exposure to $CHCl_3$ vapor. Samples with lower BuS contents than s-P(S-*co*-BuS)-11 were able to crystallize with the same result by immersing them into liquid $CHCl_3$. It should be mentioned that samples with BuS contents higher than 11 mol % are soluble in excess $CHCl_3$. The WAXS traces of the samples are typical for the clathrate form δ of neat s-PS that includes solvent molecules (apparently 5−14 wt % of toluene in s-PS).[15,33] A significant change of the intensities of the reflections at $2\theta = 8°$ and $2\theta = 10.5°$ appears with increasing copolymer content. For s-P(S-*co*-BuS)-4 both reflections are present. With increasing BuS content the intensity of the reflection at $2\theta = 8°$ increases and the reflection at $2\theta = 10.5°$ disappears. Additionally a reflection at $2\theta = 13.5°$ appears. A similar behavior is found for the clathrate forms (δ) of neat s-PS including different amounts of toluene.[33] In this system, the intensities of the two reflections change in the opposite way with the content of toluene. In a sample with an inclusion of only 1 wt % toluene, the reflection at $2\theta = 10°$ vanishes totally while the reflection at $2\theta = 8°$ is very strong, and also the reflection at $2\theta = 13.5°$ appears. Similar to this system, it can be assumed that the change of the intensities of the reflections in the copolymers is caused by the inclusion of different amounts of $CHCl_3$. An increasing BuS content reduces the inclusion of higher amounts of solvent into a stable clathrate modification, and finally s-P(S-*co*-BuS)-40 cannot be crystallized. For copolymers with a BuS content of 11, 20, and 27 mol %, the vapor-induced crystallization yields higher degrees of crystallinity than any other

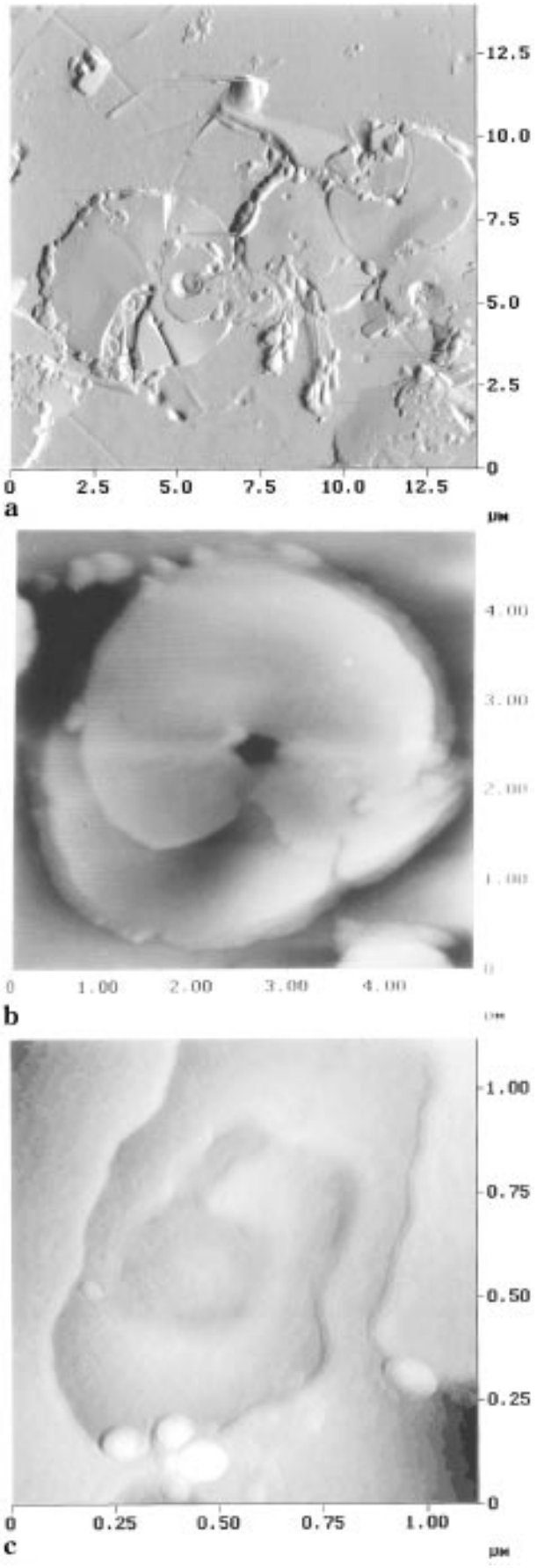

Figure 8. AFM micrographs of s-P(S-*co*-BuS)-7 isothermally crystallized at 205 °C: (a) circular crystalline entities (TMAM); (b) one single crystal enlarged (TMHM); (c) giant screw dislocation, which is visible in the center of the circular entity (TMAM).

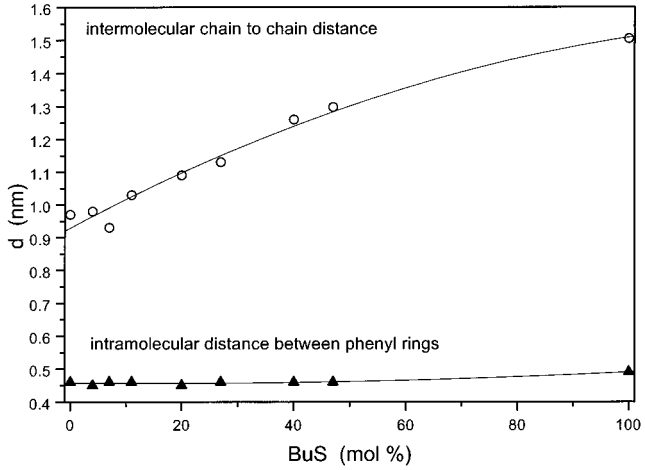

Figure 9. Intermolecular chain to chain distance and intramolecular distances between the phenyl rings calculated from the position of the two maxima of the amorphous halos in the WAXS traces as a function of the copolymer content.

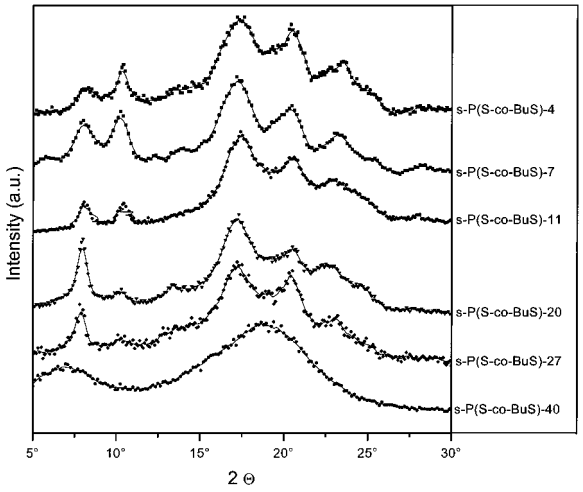

Figure 10. WAXS traces of the originally amorphous samples after $CHCl_3$ vapor induced crystallization at room temperature for 2 days.

method described in this work. Also other solvents as *n*-hexane or toluene can be used for the formation of the clathrate modification in the crystallizable copolymers.

At elevated temperatures (e.g. at 120 °C) the clathrate modifications (δ) of the copolymers with 4 and 7 mol % BuS show a transition to the solvent-free γ-modification as known for s-PS.[15] There does not exist any transition of this kind for copolymers with a higher BuS content. Figure 11 shows WAXS traces of s-P(S-*co*-BuS)-11 that is crystallized by exposing an amorphous film to $CHCl_3$ vapor at room temperature (bottom trace). The sample is originally crystallized in the δ-modification. Upon heating, the δ-modification melts in the temperature range between 102 and 112 °C. The sample does not show any transition to the γ-modification.

An AFM micrograph of s-P(S-*co*-BuS)-7 after vapor-induced crystallization can be seen in Figure 12. After treatment of the sample with $CHCl_3$ vapor, a granular morphology is visible. Granular crystalline structures are also found, e.g., for linear low density polyethylene, and they are assumed to be formed by fringed micells.[34] These morphologies were not observable prior to solvent vapor exposure of the samples.

Another method to crystallize quenched amorphous samples is cold crystallization, i.e., thermal annealing below the melting point but well above the glass

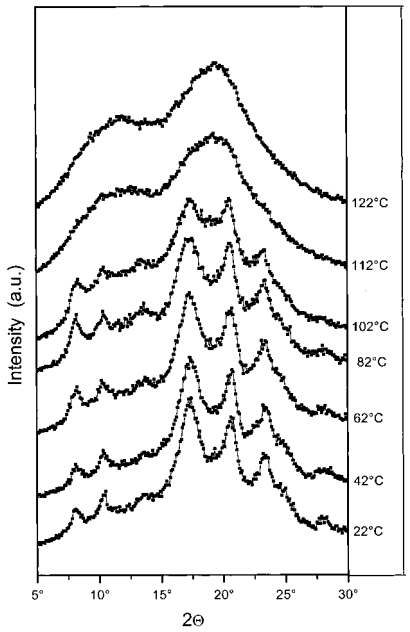

Figure 11. WAXS traces of the s-P(S-*co*-BuS)-11 after solvent-induced crystallization in $CHCl_3$ vapor taken at different temperatures.

transition temperature. Figure 13 depicts WAXS patterns of originally quenched amorphous films of s-P(S-*co*-BuS)-4 and s-P(S-*co*-BuS)-7 that are cold crystallized at 150 °C. The WAXS pattern of s-P(S-*co*-BuS)-4 shows an intermediate disordered modification between the limit ordered α″ and the limit disordered α′-forms, with small amounts of the β-modification, whereas s-P(S-*co*-BuS)-7 crystallizes exclusively in the α-modification.[14,15,17] The formation of the α-modification by thermal treatment of amorphous films is similar to the behavior of s-PS homopolymer. Copolymers with a higher BuS content cannot be crystallized from completely amorphous samples by thermal treatments of any regime.

Crystallization of Syndiotactic Poly(*p*-*n*-butylstyrene). s-P(BuS) is crystallizable from the melt and by cold crystallization. The melting point is significantly lower than that of s-PS. Determined by Hoffmann−Weeks plots, the equilibrium melting point is found to be 162 °C. Compared to s-PS the rate of crystallization of s-P(BuS) is drastically reduced at comparable supercoolings. A space filling crystallization from the melt takes 3 days in the best case. Only low degrees of crystallinity can be achieved no matter what crystallization conditions are applied. Figure 14 shows WAXS traces of s-P(BuS). The upper three traces are taken after isothermal crystallization from the melt at $T_c = 65$, 100, and 108 °C. The reflections are very sharp. Two unique modifications are observable: type I, after isothermal crystallization at 65 °C; type II at crystallization temperatures above 100 °C. The second WAXS trace from the bottom is measured after thermally induced crystallization (cold crystallization) at 100 °C of a quenched s-P(BuS) sample. The WAXS pattern is identical with that obtained after a temperature jump from the melt to the same temperature (type II). The bottom trace is the WAXS pattern of as-prepared s-P(BuS). It shows exclusively the type I modification.

Conclusion

It is found that styrene and *p*-*n*-butylstyrene can be copolymerized using the catalyst system $CpTiCl_3$/MAO. The resulting copolymers have a syndiotactic microstructure. Copolymerizations with variation of comonomer molar ratios revealed higher tendency for BuS incorporation with respect to styrene incorporation resulting in copolymerization parameters of $r_{BuS} = 1.2$ and $r_S = 0.52$. The incorporation of BuS in the s-PS chain has a large influence on the crystallization behavior. Copolymers up to a BuS content of 27 mol % are crystallizable in the presence of solvent. Under these conditions the δ-modification is formed. A δ-γ transition upon heating is observed for s-P(S-*co*-BuS)-4 and s-P(S-*co*-BuS)-7. In contrast to s-PS homopolymer, copolymers with a comonomer content of 11 mol % or higher do not show a δ-γ transition. Only copolymers with relatively low comonomer content (4 and 7 mol % BuS) are crystallizable from the melt. The copolymers have higher contents of the α-modification than neat s-PS at comparable supercoolings and also at identical crystallization temperatures. Crystallized at relatively low supercoolings the copolymers form crystalline slices

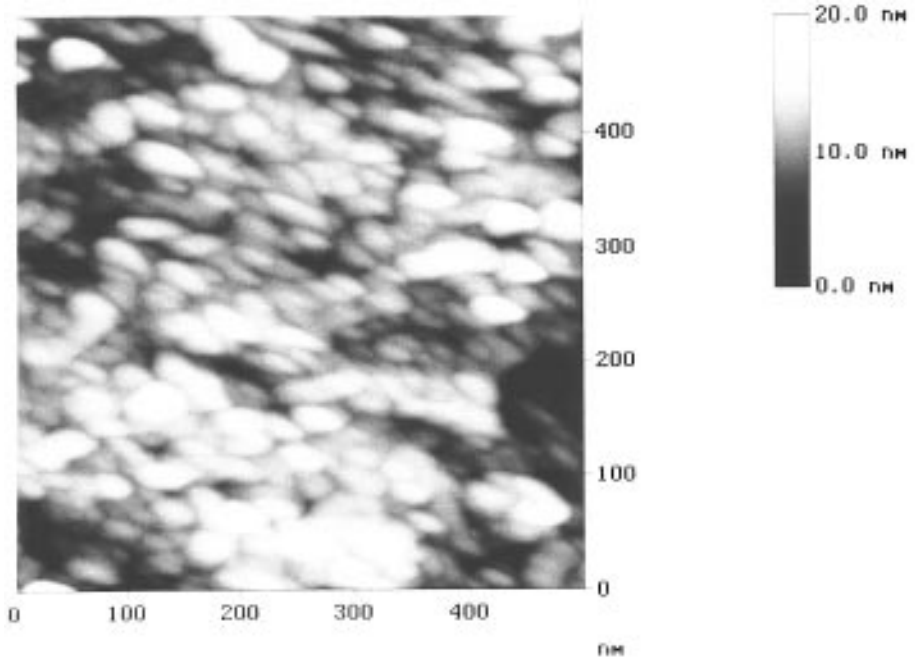

Figure 12. AFM micrograph of s-P(S-*co*-BuS)-4 after solvent-induced crystallization in $CHCl_3$ vapor (TMHM).

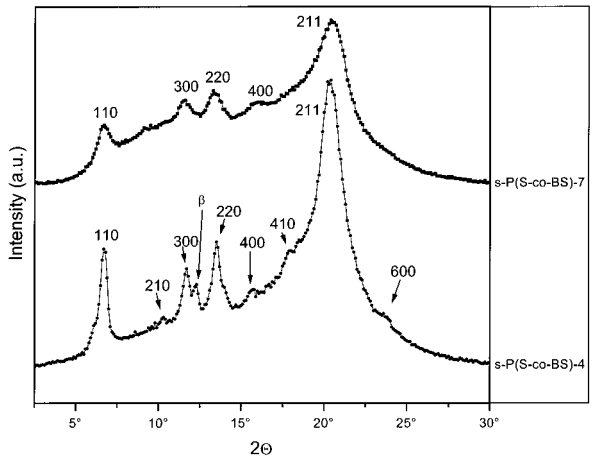

Figure 13. WAXS traces of s-P(S-*co*-BuS)-4 and s-P(S-*co*-BuS)-7 after cold crystallization of quenched amorphous films at 150 °C.

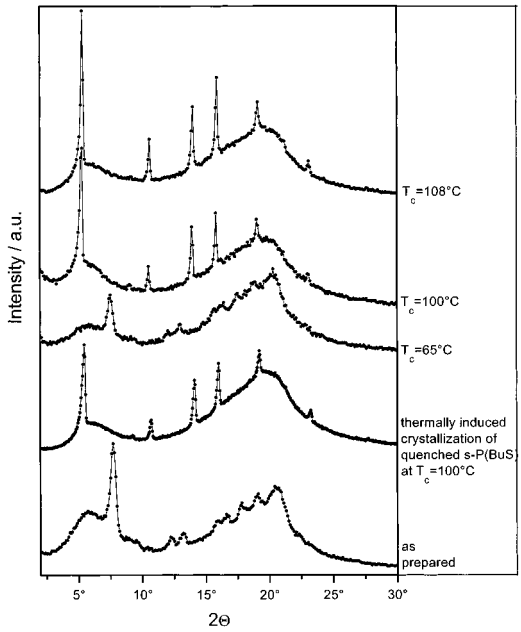

Figure 14. WAXS traces of s-P(BuS) after isothermal crystallization from the melt at T_c = 65, 100, and 108 °C, after cold crystallization of quenched s-P(BuS) at 100 °C and of as-prepared s-P(BuS).

built up by broad lamellae. Furthermore, circular objects are formed as a result of giant screw dislocations. The neat s-P(BuS) is also crystallizable. It shows two unique modifications with a distinct WAXS pattern. Type I is obtained by crystallization at large supercoolings; type II is obtained at lower supercoolings.

Acknowledgment. This work was supported by the *Bundesministerium für Bildung und Forschung* (Project No. 03M40719). The authors also thank the BASF AG for financial support and Witco AG for providing samples of MAO. F.G.S. is grateful for a fellowship from the *Studienstiftung des deutschen Volkes*.

References and Notes

(1) Ishihara, N.; Seimiya, T.; Kuramoto, M.; Uoi, M. *Macromolecules* **1986**, *19*, 2465..
(2) (a) Zambelli, A.; Longo, P.; Pellecchia, C.; Grassi, A. *Macromolecules* **1987**, *20*, 2035. (b) Pellecchia, C.; Longo, P.; Grassi, A.; Ammendola, P.; Zambelli, A. *Macromol. Rapid. Commun.* **1987**, *8*, 277.
(3) (a) Grassi, A.; Pellecchia, C.; Longo, P.; Zambelli, A. *Gazz. Chim. Ital.* **1987**, *117*, 249. (b) Ammendola, P.; Pellecchia, C.; Longo, P.; Zambelli, A. *Gazz. Chim. Ital.* **1987**, *117*, 65.
(4) Ishihara, N.; Kuramoto, M.; Uoi, M. *Macromolecules* **1988**, *21*, 3356.
(5) Dall'Occo, T.; Sartori, F.; Vecellio, G.; Zucchini, A.; Maldotti, A. *Macromol. Chem. Phys.* **1993**, *194*, 151.
(6) (a) Zambelli, A.; Oliva, L.; Pellecchia, C. *Macromolecules* **1989**, *22*, 2129. (b) Pellecchia, C.; Longo, P.; Proto, A.; Zambelli, A. *Macromol. Rapid. Commun.* **1992**, *13*, 265.
(7) Kakugo, M.; Miyatake, T.; Mizunuma, K. *Stud. Surf. Sci. Catal.* **1990**, *56*, 517.
(8) Kucht, A.; Kucht, H.; Barry, S.; Chien, J. C. W.; Rausch, M. D. *Organometallics* **1993**, *12*, 3075.
(9) Kaminsky, W.; Lenk, S. *Macromol. Chem. Phys.* **1994**, *195*, 2093.
(10) (a) Pellecchia, C.; Pappalardo, D.; Oliva, L.; Zambelli, A. *J. Am. Chem. Soc.* **1995**, *117*, 6593. (b) Longo, P.; Grassi, A.; Proto, A.; Ammendola, P. *Macromolecules* **1988**, *21*, 24.
(11) Grassi, A.; Longo, P.; Proto, A.; Zambelli, A. *Macromolecules* **1989**, *22*, 104.
(12) Soga, K.; Nakatani, H.; Monoi, T. *Macromolecules* **1990**, *23*, 953.
(13) De Rosa, C.; Rapacciuolo, M.; Guerra, G.; Petraccone, V.; Corradini, P. *Polymer* **1992**, *23*, 1423.
(14) De Rosa, C.; Guerra, G.; Petraccone, V.; Corradini, P. *Polym. J.* **1991**, *23*, 1435.
(15) Guerra, G.; Vitagliano, M.; De Rosa, C.; Petraccone, V.; Corradini, P. *Macromolecules* **1990**, *23*, 1539.
(16) Natta, G.; Corradini, P. *Makromol. Chem.* **1955**, *16*, 77.
(17) De Rosa, C. *Macromolecules* **1996**, *26*, 8460.
(18) De Rosa, C.; Petraccone, V.; Dal Poggetto, F.; Guerra, G.; Pirozzi, B.; Di Lorenzo, M. L.; Corradini, P. *Macromolecules* **1995**, *28*, 5507.
(19) Manfredi, C.; Guerra, G.; De Rosa, C.; Busico, V.; Corradini, P. *Macromolecules* **1995**, *28*, 6508.
(20) Thomann, R.; Wang, C.; Kressler, J.; Mülhaupt, R. *Macromolecules* **1996**, *29*, 8425.
(21) Wunderlich B. *Macromolecular Physics,* 1st ed.; Academic Press: New York, 1979; Vol. 1.
(22) Barnes, J. D.; McKenna, G. B.; Landes, B. G.; Bubeck, R. A.; Banks, D. *SPE ANTEC 96*, Indianapolis, IN, 1996; p 1532.
(23) (a) Karol, F. J.; Kao, S. C.; Cann, K. J. *J. Polym. Sci., Part A: Polym. Chem.* **1993**, *31*, 2541. (b) Jaber, I. A.; Fink, G. *Macromol. Chem. Phys.* **1994** *195*, 2491. (c) Koivumäki, J.; Fink, G.; Seppälä, J. V. *Macromolecules* **1994**, *27*, 6254.
(24) (a) Owens, F. H.; Pellmann, R. P.; Zimmermann, F. E. *J. Org. Chem* **1960**, *25*, 1808. (b) Nystrom, R. F.; Berger, C. R. A. J. Am. Soc. **1958**, *80*, 2896. (c) *Organikum*, 18th ed.;VEB Deutscher Verlag der Wissenschaft: Berlin, 1990.
(25) Wunderlich B. *Macromolecular Physics;* 1st ed.; Academic Press: New York, 1980; Vol. 3.
(26) Hoffman, J. D.; Weeks J. J. *J. Res. Natl. Bur. Stand.* **1962**, *A33*, 13.
(27) DiCorleto, J. A.; Bassett, D. C. *Polymer* **1990**, *31*, 1971.
(28) Krimm, S. *J. Phys. Chem.* **1953**, *57*, 22.
(29) Bjornhang, A.; Ellefsen, O.; Tonnersen B. A. *J. Polym. Sci.* **1954**, *12*, 621.
(30) Kilian, H. G.; Boueche, K. *J. Polym. Sci* .**1954**, *58*, 311.
(31) Krimm, S.; Tobolsky, A. V. *Text. Res. J.* **1951**, *21*, 805.
(32) Katz, J. R. *Trans. Faraday. Soc.* **1936**, *32*, 77.
(33) De Rosa, C.; Guerra, G.; Petraccone, V.; Pirozzi, B. *Macromolecules* **1997**, *30*, 4147.
(34) Minick, J.; Moet, A.; Hiltner, A.; Baer, E.; Chum, S. P. *J. Appl. Polym. Sci.* **1995**, *58*, 1371.

MA9711856